



Published in final edited form as:

Mol Genet Metab. 2019 May ; 127(1): 95–106. doi:10.1016/j.ymgme.2018.11.015.

ATP13A2 missense variant in Australian Cattle Dogs with late onset neuronal ceroid lipofuscinosis

Isabelle Schmutz^a, Vidhya Jagannathan^a, Florian Bartenschlager^b, Veronika M. Stein^c, Achim D. Gruber^b, Tosso Leeb^a, Martin L. Katz^{d,*}

^aInstitute of Genetics, Vetsuisse Faculty, University of Bern, 3001 Bern, Switzerland

^bDepartment of Veterinary Pathology, College of Veterinary Medicine, Freie Universität Berlin, 14163 Berlin, Germany

^cDepartment of Clinical Veterinary Sciences, Vetsuisse Faculty, University of Bern, CH-3012 Bern, Switzerland

^dMason Eye Institute, University of Missouri School of Medicine, Columbia, MO, USA

Abstract

The neuronal ceroid lipofuscinoses (NCLs) are lysosomal storage disorders characterized by progressive neurodegeneration and declines in neurological functions. Pathogenic sequence variants in at least 13 genes underlie different forms of NCL, almost all of which are recessively inherited. To date 13 sequence variants in 8 canine orthologs of human NCL genes have been found to occur in 11 dog breeds in which they result in progressive neurological disorders similar to human NCLs. Canine NCLs can serve as models for preclinical evaluation of therapeutic interventions for these disorders. In most NCLs, the onset of neurological signs occurs in childhood, but some forms have adult onsets. Among these is CLN12 disease, also known as Kufor-Rakeb syndrome, PARK9, and spastic paraplegia⁷⁸. These disorders result from variants in *ATP13A2* which encodes a putative trans-membrane ion transporter important for lysosomal function. Three Australian Cattle Dogs (a female and two of her offspring) were identified with a progressive neurological disorder with an onset of clinical signs at approximately 6 years of age. The affected dogs exhibited clinical courses and histopathology characteristic of the NCLs. Whole genome sequence analysis of one of these dogs revealed a homozygous c.1118C > T variant in *ATP13A2* that predicts a nonconservative p.(Thr373Ile) amino acid substitution. All 3 affected dogs were homozygous for this variant, which was heterozygous in 42 of 394 unaffected Australian Cattle Dogs, the remainder of which were homozygous for the c.1118C allele. The high frequency of the mutant allele in this breed suggests that further screening for this variant should identify additional homozygous dogs and indicates that it would be advisable to perform such screening prior to breeding Australian Cattle Dogs.

This is an open access article under the CC BY-NC-ND license (<http://creativecommons.org/licenses/by-nc-nd/4.0/>).

*Corresponding author at: Mason Eye Institute, Room EC-203, University of Missouri School of Medicine, Columbia, MO 65121, USA. katzm@health.missouri.edu (M.L. Katz).

Appendix A. Supplementary data

Supplementary data to this article can be found online at <https://doi.org/10.1016/j.ymgme.2018.11.015>.

Keywords

Canis lupus familiaris; Animal model; Whole genome sequencing; Neuronal ceroid lipofuscinosis; Lysosomal storage disease; Neurodegeneration; Dog; CLN12; Kufor-Rakeb syndrome; PARK9; Spastic paraplegia

1. Introduction

Dogs suffer from many of the same hereditary progressive neuro-degenerative diseases that occur in humans. Among these are a group of disorders designated the neuronal ceroid lipofuscinoses (NCLs). In people these diseases are characterized by apparently normal development followed by progressive declines in cognitive and motor functions, loss of vision, seizures, and in most cases premature death [1]. These clinical signs are accompanied by progressive degeneration of the central nervous system and usually the retina as well. The human NCLs are designated CLN1 through CLN14 based on the gene in which the pathological sequence variant occurs. DNA sequence variants that underlie the NCLs occur in at least 13 genes [2] (Table S1). The ages of onset of clinical signs and the rates of disease progression vary depending on the gene in which the causative variant occurs and the nature of the variant [3]. The disease phenotype can vary substantially with each form of NCL [1]. Onset of disease signs ranges from infancy to adulthood.

Diseases with clinical signs similar to the human NCLs have been reported in over 20 dog breeds [4,5]. The causes of the majority of these canine disorders have been found to be variants in the canine orthologs of genes associated with human NCLs. To date, sequence variants in 9 canine orthologs of human NCL genes have been associated with NCLs in dogs [4,5]. Among these are diseases with onset of clinical signs ranging from a few months to 7 years of age.

Australian Cattle Dogs are one of the breeds affected by NCL for which a genetic basis has been identified. The disease-causing genetic variant identified in the breed is a truncating nonsense variant in *CLN5* [6]. This same variant causes NCL disease in Border Collies [7]. The onset of clinical signs in dogs with this variant becomes apparent around the age of 12 months and affected dogs reach end-stage disease with severe neurological signs at 20 to 27 months of age. Three closely-related Australian Cattle Dogs presented with progressive neurological signs typical of the NCLs that did not become apparent until the dogs were approximately 6 years of age with disease progression from onset to end-stage of up to more than 2 years. None of these dogs had the *CLN5* sequence variant previously associated with NCL in this breed. Studies were therefore undertaken to determine whether these dogs suffered from another form of NCL, and to determine whether their disease was associated with a sequence variant in one of the known NCL genes.

2. Materials and methods

2.1. Ethics statement

The dogs in this study were examined and blood and tissue samples were collected with the consent of their owners. The studies were performed with the approval of the

Cantonal Committee for Animal Experiments (Canton of Bern; permit BE75/16). All animal experiments were done in accordance with local laws and regulations including the U.S. National Institutes of Health Guide for the Care and Use of Laboratory Animals.

2.2. Animals

This study included 397 Australian Cattle dogs. Three closely related dogs presented clinical signs characteristic of NCL and were designated as cases. These signs are described in detail in the Results section of this paper. The three affected Australian Cattle Dogs in this study consisted of a female (dog A) and two offspring from one of her litters (one male [dog B] and one female [dog C]). Also included is dog D, the father of dogs B and C. DNA samples from the remaining 393 Australian Cattle Dogs were collected in the context of other ongoing research projects. They included 26 Australian Cattle Dogs older than 6 years that did not show any signs of neurological disease and 367 Australian Cattle Dogs, for which no phenotype information was available and which were considered population controls. Samples which had been donated to the Vetsuisse Biobank from 555 additional dogs of 70 diverse breeds were also used as controls (Table S2). Genomic DNA was extracted from whole blood of each of these dogs.

2.3. Disease phenotype characterization

Characterization of the behavioral abnormalities in the three affected dogs was based primarily on information provided by the dogs' owners on a symptom survey form that has been in use for over 10 years for identifying dogs with various forms of NCL or by information provided by the owners in a similar manner. Dog A was euthanized at the age of 8 years and 2 months due to the progression of disease signs. Before her death, blood was obtained for DNA isolation, but no tissues were collected at the time of euthanasia. Dogs B and C were euthanized at the age of 6 years and 9 months and at 7 years and 7 months respectively due to progression of disease signs, and tissues were collected at the time of euthanasia, as described below. Dog D lived to the age of 16 years and did not exhibit any behavioral or neurological abnormalities.

At the time of euthanasia, samples of cerebellum, parietal cerebral cortex, eyes, and heart ventricular wall were collected from dogs B and C and a section of cervical spinal cord was collected from dog C. From each dog, one eye and a portion of each other tissue was fixed in 10% buffered formalin or "immuno fix" (3.5% paraformaldehyde, 0.05% glutaraldehyde, 120 mM sodium cacodylate, 1 mM CaCl₂, pH 7.4), and the other eye and a portion of each other tissue was fixed in cacodylatebuffered glutaraldehyde or glutaraldehyde-paraformaldehyde [8]. The formalin and "Immuno"-fixed tissues were embedded in paraffin or Tissue-Tek embedding medium (Sakura Finetek, Tokyo, Japan) and sections were cut and stained as described in the Results section. Immunostaining of paraffin sections for the lysosomal marker LAMP1 was performed with a polyclonal rabbit anti-LAMP1 primary antibody (Abcam ab24170) using previously described techniques [9]. In addition, unstained sections of the paraffin-embedded samples were deparaffinized and examined unstained with fluorescence microscopy as described previously, as were cryosections of the Tissue-Tek embedded samples [10]. Cryosections of cardiac muscle samples were also examined after staining with the lipid dye Sudan Black III and counter-staining with Mayer's Hematoxylin.

Portions of the glutaraldehydefixed tissues were post-fixed in osmium tetroxide, embedded in epoxy resin and 70 to 90 nm thick sections were cut from the embedded samples. The sections were collected on 200 mesh thin-barred copper grids, stained with uranyl acetate and lead citrate, and were then examined and photographed with a JEOL 1400 transmission electron microscope equipped with a Gatan digital microscope. Sections of the resin-embedded tissues were also cut at a thickness of 0.4 to 0.8 μm , mounted on glass slides, stained with toluidine blue, and photographed with conventional transmitted light microscopy.

2.4. Reference sequences

All analyses were performed using the dog CanFam 3.1 genome assembly as reference sequence. Numbering within the canine *ATP13A2* gene refers to NCBI RefSeq accessions [XM_005617949.3](#) (mRNA) and [XP_005618006.1](#) (protein). Numbering within the human *ATP13A2* gene refers to NCBI RefSeq accessions [NM_022089.3](#) (mRNA) and [NP_071372.1](#) (protein).

2.5. Whole genome resequencing and variant filtering

An Illumina TruSeq PCR-free library with an insert size of 350 bp was prepared from one affected Australian Cattle dog (dog B) and 195 million 2×150 bp paired-end reads were obtained on an Illumina HiSeq 3000 instrument ($21.6\times$ coverage). Mapping and variant calling was done as described [11]. The sequence data were deposited under study accession PRJEB16012 and sample accession SAMEA104500413 at the European Nucleotide Archive. Functional effects and genomic context of the called variants were annotated using SnpEff software [12] together with the NCBI *Canis lupus familiaris* Annotation Release 104. For private variant filtering we used control genome sequences from 8 wolves and 209 dogs. These genomes were either publicly available [13] or produced during other previous projects in our laboratory (Table S3).

2.6. DNA extraction, PCR and Sanger sequencing

Genomic DNA was extracted from EDTA blood samples using the Maxwell RSC Whole Blood DNA Kit in combination with the Maxwell RSC machine (Promega). We used a Sanger sequencing protocol for targeted genotyping of the *ATP13A2*:c.1118C > T variant. Specifically, a 593 bp PCR product was amplified from genomic DNA using the AmpliTaqGold360Mastermix (Life Technologies) together with primers 5'-GAT GCC TGC ATG TAT GGT TG-3' (forward) and 5'-GTG GGC GGT TTC ACT TTT TA-3' (reverse). After treatment with exonuclease I and alkaline phosphatase, amplicons were sequenced on an ABI 3730 DNA Analyzer (Life Technologies). Sanger sequences were analyzed with the Sequencher 5.1 software (GeneCodes).

3. Results

3.1. Characterization of disease phenotype

The onset of neurological signs in the affected dogs occurred at approximately 6 years of age and progressively worsened over time. Among the disease-related signs reported by the dogs' owners were anxiety, impaired ability to recognize and respond to previously

learned commands, increased sensitivity to loud or unexpected sounds, sleep disturbances, inappropriate or persistent vocalization, impaired ability to navigate stairs and to jump up or down from furniture, trembling, seizures, stiffness or weakness, loss of coordination, and ability to see in both bright and dim light. In addition to these signs, neurological examination findings in affected dog C included hypersensitivity to tactile stimuli, clumsiness, a broad-based stance in the pelvic limbs, mild ataxia, unsteady gait on slippery surfaces, intermittent pacing gait, hopping gait in pelvic limbs while trotting, reduced palpebral reflex and reduced menace response in both eyes, normal pupillary light reflexes in response to bright stimuli, and decreased nasal sensation. In addition, the affected dog that underwent a neurologic exam exhibited slightly delayed proprioception in the pelvic limbs, delayed and reduced hopping in all 4 limbs, and reduced extensor postural thrust. Spinal reflexes were normal. Dog B was euthanized at age 6 years and 9 months, and his littermate dog C was euthanized at age 7 years and 8 months due to the progression of these signs. Dog A, the mother of dogs B and C, was euthanized at age 8 years and 2 months. In addition to exhibiting the signs described above, she became very aggressive starting at about 8 years of age to the point of being dangerous, even toward her owner, and euthanasia was elected for this reason. Dog D, the father of dogs B and C, lived to be 16 years of age without exhibiting any of these behavioral abnormalities.

Although the behavioral signs exhibited by the affected dogs are consistent with the canine NCLs, other causes are possible, including other inherited neurological diseases or brain tumors. A universal characteristic of both canine and human NCLs is the progressive accumulation of autofluorescent lysosomal storage bodies in cells of the central nervous system, as well as many other tissues [1]. The presence of these storage bodies can be used to distinguish the NCLs from other neurological disorders. Therefore, unstained sections of brain, retina, and heart from affected dogs B and C were examined for the presence of these characteristic autofluorescent storage bodies.

The cerebellum of dogs B and C exhibited massive accumulations of autofluorescent storage bodies primarily in the Purkinje cell layer, the meninges and large neurons in the deep cerebellar nuclei (Fig. 1). These autofluorescent aggregates were also present to a lesser extent in the molecular layer of the cerebellar cortex. In the Purkinje cell layer autofluorescent inclusions were abundant within the perinuclear areas of the Purkinje cells (Fig. 1A), as well as in clumps much larger than typical Purkinje cell bodies (Fig. 1B). Abundant autofluorescent storage material was also present in the cerebellar meninges (Fig. 1C). Massive accumulations of the storage bodies in the deep cerebellar nuclei were localized to the perinuclear regions of large neurons (Fig. 1D).

In the cerebral cortex of both affected littermates, autofluorescent storage material was present in almost all neurons (Fig. 2). This material appeared as aggregates of small granules in the perinuclear regions of the cells. When the neurons were cut in the appropriate plane of section, these aggregates could be seen to be concentrated in one region of the cell body rather than being evenly distributed throughout the cell (Fig. 2B). Neurons in both the ventral and dorsal horns of the cervical spinal cord of dog C contained massive amounts of auto-fluorescent storage material (Fig. 3). As in other forms of canine NCL, disease-specific autofluorescent material was observed in retinal ganglion cells and along the outer limiting

membrane from affected dog C (Fig. 4A). At the electron microscopic level, the storage material in the ganglion cells consisted on membrane-bounded inclusions containing whorls of condensed membrane-like structures sometimes embedded in a granular matrix (Fig. 4).

As in some other forms of canine NCL, strands of autofluorescent storage bodies were present between the muscle fibers of the cardiac muscle (Fig. 5A). Based on their location and topography, it appears that these storage bodies are located in the cardiac Purkinje fibers. Substantial aggregates of autofluorescent storage bodies were also present in the neurons of cardiac ganglia (Fig. 5B).

The ultrastructural appearances of the disease-related cellular inclusion bodies in the tissues of affected dog B were quite distinctive. In the cerebellar Purkinje layer, these consisted of membrane-bounded structures as large as 4 to 5 μm in diameter (Fig. 6). The contents of most of these inclusions consisted primarily of whorls and stacks of membrane-like structures (Fig. 6A). However the contents of some inclusion bodies consisted largely of curvilinear material similar that which is characteristic of the storage material typical of the CLN12 form of NCL (arrows in Fig. 6A). A small minority of the inclusion bodies in the cerebellum consisted of tightly packed fine membrane-like material that was randomly oriented (arrowhead in Fig. 6B).

The contents of the membrane-bounded disease-related inclusions in cerebral cortical neurons of the affected dogs consisted primarily of clusters of membrane-like structures, much like those in the cerebellum (Fig. 7). However, for the most part these clusters did not occur in the whorl-like arrangements observed in the cerebellum. The sizes and shapes of the individual inclusion bodies were variable and range about 3 to as much as 20 μm in diameter. No inclusions with curvilinear contents were observed in the cerebral cortical samples, but some of the storage bodies contained scattered dark amorphous inclusions that were 0.5 to 1 μm in diameter.

The ultrastructural appearances of the disease-related auto-fluorescent inclusions of the cardiac muscle from the affected dog were quite different from those of the inclusions present in the brain. The disease-related inclusions in the cardiac muscle consisted of tightly-packed aggregates of membrane-bounded rounded structures and structures that appear to have been round but to have been compressed into other shapes by crowding from the surrounding inclusion bodies (Fig. 8). These inclusions consisted of a mixture of two distinctly different types based on the appearance of their contents. The contents of some of the storage bodies had a uniform electron-dense appearance with no structural detail. The contents of the remaining inclusions consisted of uniform flocculent material. The two types of inclusions were randomly intermixed and ranged in size from less than 0.2 μm to greater than 6 μm . No nerve ganglia were present in the cardiac samples that were preserved for electron microscopic examination.

The ultrastructural appearances of the uniformly electron dense structures within the cardiac muscle inclusions are typical of lipid droplets [14]. Indeed, these structures stained with the lipid stain Sudan Black III in cryostat sections of cardiac muscle (Fig. 9A), whereas the disease-related inclusion bodies in neural tissues did not stain with this dye. Within

the inclusions in the heart, a subset of the granular particles stained with the periodic acid-Schiff (PAS) reagent, which is specific for the carbohydrate moieties of polysaccharides, glycoproteins, and glycolipids (Fig. 9B). The staining pattern in the heart suggested that only the structures with flocculent material and not the lipid droplet-like structures contained carbohydrate components. The disease-specific inclusions in the cardiac muscle also exhibited LAMP1 immunostaining (Fig. 9C) indicating that these inclusions were derived from lysosomes. The disease-specific cellular inclusion bodies in cerebral cortex and cerebellum also stained strongly with PAS, but those in the retina did not (data not shown). As with the cardiac muscle, the disease-specific cellular inclusions in the cerebral cortex, cerebellum and retinal ganglion cells stained with an anti-LAMP1 antibody (Fig. 10), suggesting that these inclusions were also derived from lysosomes.

In addition to exhibiting a characteristic autofluorescence, the storage material that accumulates in many of the NCLs has been shown to stain with Luxol fast blue in paraffin sections [15–17]. This was also the case for the storage bodies in every tissue from affected dog B that was examined (Fig. 11). Within the Purkinje cell layer were clusters of cells variable in shape and size that were filled with autofluorescent material (Fig. 1B) that stained intensely with Luxol fast blue (g in Fig. 11B). These cells may be microglia-derived phagocytic cells (gitter cells) that have taken up large amounts of storage material that originated in Purkinje cells that have degenerated. Non-Purkinje cells in or near the Purkinje cell layer that contain disease-related storage material have been reported in other forms of canine NCL [6,18], and a similar clustering of these cells in the Purkinje layer of the cerebellum occurs in at least one of these other NCLs [6]. Whether these cells represent phagocytic cells that have taken up storage material originally generated in Purkinje cells remains to be determined.

In earlier-onset forms of canine as well as human NCL, the diseases are characterized by pronounced astrogliosis [6,18–21]. Immunostaining (IHC) of brain and retinal tissues of the affected Australian Cattle Dogs for glial fibrillary acid protein (GFAP), a marker for reactive astrocytes, indicated that astrogliosis is also a prominent feature of this late-onset disease, although not in the cerebellar cortex (Figs. 12 and 13). In addition, pronounced GFAP immunostaining was observed in small number of cells adjacent to large blood vessels in heart ventricular muscle and surrounding large blood vessels in the inner retina (Fig. 13).

3.2. Genetic analysis

We performed whole genome sequencing on one affected offspring and searched for private heterozygous and homozygous protein-changing variants in the case by comparing them with genome sequences from 8 wolves and 209 dogs from genetically diverse breeds (Table S3). We did not have any specific information regarding a potential NCL phenotype in the controls. However, as this is a rare condition, we assumed the control dogs and wolves to be homozygous wildtype at the causative variant.

The variant calling pipeline detected 4,028,278 variants in the genome of the sequenced case. Of these, 151 were absent from the control genomes and predicted to be protein-changing. We prioritized 13 known candidate genes, which had previously been identified in human and animal neuronal ceroid lipofuscinoses (Table S1). Only one variant was

located in one of these candidate genes (*ATP13A2*), while the other 150 were in genes that we did not consider to be likely functional candidate genes (Table 1; Table S4). The *ATP13A2* variant was a missense variant, XM_005617949.3:c.1118C > T, predicted to result in a non-conservative exchange of a threonine into an isoleucine, XP_005618006.1:p.(Thr373Ile). The predicted amino acid substitution is located in the cytoplasmic E1-E2 ATPase domain (pfam00122). The wildtype threonine is conserved in *ATP13A2* orthologs across phylo-genetically diverse vertebrates (Fig. 14).

We then genotyped the variant in a cohort of 397 Australian Cattle Dogs, which included the 3 known cases, dog D, 26 unaffected Australian Cattle Dogs older than 6 years of age and 367 population controls. This revealed a perfect association of the genotypes with the phenotype (Table 2). All three affected dogs carried the variant in homozygous state. Dog D, the sire of the two affected dogs was heterozygous (obligate carrier). Among the other 393 Australian Cattle dogs, we observed 352 dogs that were homozygous wildtype and 41 dogs that were heterozygous and presumably carriers for the disease. These data indicate that among the Australian Cattle Dogs that were sampled, the carrier frequency is around 10%. Because of sampling bias in our population, the carrier frequency among all Australian Cattle Dogs may be different. We also genotyped 555 dogs from genetically diverse breeds. None of these dogs carried the *ATP13A2*:c.1118C > T variant (Table S2).

4. Discussion and conclusions

A human autosomal recessive neurological disorder originally named Kufor-Rakeb syndrome (KRS) was first described in 1994 in members of a consanguineous Arabic family in which five siblings were affected [22]. The disease name was based on the name of the region in Jordan where the family resided. The onset of disease signs occurred at 12 to 16 years of age and progressively worsened over time resulting in severe impairment of motor and cognitive functions within 2 years of onset. Initial signs were abnormal facial expressions and progressive slowing of all motor functions. The disease progression is characterized by development of levodopa-responsive parkinsonism (severe akinesia and rigidity), supranuclear upgaze paresis, constant drooling, speech impairment, and dementia. The most severely affected individuals were bedridden with a generalized flexed posture. All of the affected siblings had normal visual acuity and no retinal abnormalities were observed with fundoscopy. Significant atrophy of the globus pallidus and the pyramids, as well as generalized brain atrophy in later stages of disease progression were documented with magnetic resonance imaging. The disease was quite slow, but ultimately affected individuals died as a result of profound neurological decline. There was significant variability in the severity of clinical signs between the affected siblings. A causal genetic variant for this disorder was found to be a 22 bp deletion in exon 16 of *ATP13A2* [23].

Subsequently, over 140 sequence variants in the coding regions of *ATP13A2* have been identified in people, many of which have been reported to pathogenic (<https://www.ncbi.nlm.nih.gov/clinvar>) [11,24–31]. Many of the pathogenic variants predict single amino acid changes in the protein, although partial deletions and splice site variants associated with neurological disease have also been identified [32]. Among the clinical diagnoses associated with these variants, are NCL (CLN12, OMIM 610513), a

Parkinsonian-like disorder designated PARK9, and spastic paraplegia78 (OMIM 617225) [33]. Interestingly, the latter authors found that a sequence variant in another NCL gene, *TPP1*, also resulted in spastic paraplegia that was responsive to L-DOPA. This represents one of a number of overlaps between phenotypes associated with *ATP13A2* variants and variants in other NCL genes and supports the classification of *ATP13A2* pathogenic variants as NCL types. In most cases of neurologic disease associated with a variety of *ATP13A2* sequence variants, at least some of the signs were typical of recognized NCL disorders, including diffuse brain atrophy, myoclonus, progressive cognitive decline, tremor, hallucinations, and behavioral abnormalities. For more detailed information and citations to relevant publications, see OMIM entry 610,513.

The spectrum of clinical signs associated with these mutations varies both among individuals homozygous for the same variant and between individuals with different variants in *ATP13A2* [34–36]. The bases for this heterogeneity in clinical signs is unknown, but differences in ages of disease onset, progression, and clinical signs among individuals homozygous for the same variant suggest that other genetic differences modulate the effects of abnormalities in or absence of *ATP13A2*. Environmental factors are less likely to play a significant role in this heterogeneity, since the disease phenotype can vary significantly among siblings.

Given the variability in phenotypes associated with different mutations or even with the same variant in *ATP13A2* [29], one may be tempted to assign subsets of the disorders resulting from variants in this gene to either the NCLs, Parkinsonian disorders, spastic paraplegias, or other groups depending on the phenotype, but in some cases this would result in siblings with the same variant but different phenotypes being classified as having different diseases. On the other hand, it has become the convention in the NCL field to classify diseases in this group by the gene in which the variant occurs rather than by disease phenotype. This makes sense with respect to understanding the primary disease mechanisms and potential approaches to therapy. Therefore, because of the variability in phenotypes among patients with *ATP13A2* variants, there is an advantage to grouping these disorders together under one designation based on the gene in which the causal variants occur, which we propose to be the currently accepted CLN12. As with the other NCL types, one can differentiate patients within the overall NCL groups as being “variants” of CLN12 based on phenotype. We discourage continued use of the disease names KRS, PARK9, and spastic paraplegia78 because it would be cumbersome and not particularly helpful to use a separate disease name for each different pathogenic *ATP13A2* variant. Rather, we encourage future use of CLN12 to designate all disorders resulting from pathogenic variants in *ATP13A2*, with the addition of descriptive terms related to phenotype to describe subtypes of these disorders. This practice is well established in the NCL field for all forms of NCL, so for consistency, should be applied to all disorders resulting from pathogenic variants in *ATP13A2*.

The function of the protein or proteins encoded by *ATP13A2* has not been firmly established. There is evidence that the *ATP13A2* protein is a lysosomal transmembrane ATPase ion pump that appears to be a Zn^{2+} transporter [30,31,37–40]. Variants that are predicted to alter the function of *ATP13A2* result in lysosomal dysfunction and

the accumulation of lysosomal storage bodies [11,37,40–42], as well as altering other cellular functions including endosomal trafficking and functions that either depend on intracellular zinc homeostasis or are secondary to lysosomal dysfunction [34–36]. However, experimental evidence also suggests that ATP13A2 plays a direct role in mitochondrial bioenergetics, autophagy, α -synuclein metabolism, and endosome-mediated cargo sorting [29,34–36,39,43,44]. Different pathological variants in human *ATP13A2* have different effects on the protein, including its complete absence, impaired ATPase activity, mislocation within the cell, enhanced proteosomal degradation, and increased protein stability [31]. Which of these effects are associated with the Australian Cattle Dog p.(Thr373Ile) variant remain to be determined.

The neuronal ceroid lipofuscinoses (NCLs) are a group of inherited progressive neurodegenerative disorders that are characterized by normal development followed in most cases by progressive declines in cognitive and motor functions, loss of vision, seizures, brain atrophy, retinal degeneration, and a generalized accumulation of auto-fluorescent lysosomal storage bodies throughout the central nervous system and in many other tissues [1]. Variants in at least 13 genes underlie different forms of NCL [2]. Naturally occurring NCLs have been described in many dog breeds, and the genetic bases for these disorders have been identified in genes orthologous to those associated with human NCLs [4,5]. A late-adult onset form of NCL in Tibetan Terriers was found to result from a truncating single base deletion in *ATP13A2* [45]. This deletion was associated with exon skipping in affected dogs [46]. These discoveries led to a re-evaluation of KRS associated with *ATP13A2* variants and its classification as an NCL with the designation of CLN12 [47]. The basis for this classification, in addition to the similarity in clinical signs and progressive neurodegeneration, is the finding that like other NCLs, individuals that are homozygous for variants in *ATP13A2* exhibit accumulation of auto-fluorescent lysosomal storage bodies with ultrastructural features characteristic of the NCLs.

Unlike the variability in clinical signs in human subjects with neurological diseases associated with *ATP13A2* sequence variants, even between siblings homozygous for the same variant, the disease signs and progression among Tibetan Terriers with CLN12 disease due to a single base deletion in *ATP13A2* were quite uniform [45]. The age of onset is approximately 7 years of age and neurological signs in most affected dogs progress to the stage at which euthanasia is elected at approximately 10 years of age. The clinical signs associated with the Tibetan Terrier disease only partially overlap those of human subjects with *ATP13A2*-related disease. The canine disease is characterized by anxiety, aggression, cognitive decline, loss of coordination, ataxia, tremors, seizures (primarily near disease end-stage), and progressive vision loss in both dim and bright lighting. Unlike most human subjects with *ATP13A2*-related disorders, Tibetan Terriers with CLN12 disease exhibited pronounced retinal degeneration and impaired retinal function [48].

The Tibetan Terrier disease resulted from a single base deletion (frameshift) that would be expected to result in a complete lack of ATP13A2 protein, whereas the mutant allele in the Australian Cattle Dogs is predicted to encode a p.(Thr373Ile) amino acid substitution in ATP13A2. Because the wildtype threonine is conserved in ATP13A2 orthologs across phylogenetically diverse vertebrates, and replacement of threonine by isoleucine at p.373

results in a disease phenotype very similar to that of Tibetan Terriers with the *ATP13A2* single base deletion, it appears likely that Australian Cattle Dog missense variant alters an important functional domain of the protein. This is consistent with the fact that the age of onset was earlier and the rate of disease progression was faster in the Australian Cattle Dogs than that in Tibetan Terriers with the truncating variant. Because the affected Australian Cattle Dogs are expected to produce a dysfunctional form of ATP13A2, biochemical analyses of tissues from dogs with this mutation may lead to a better understanding of the normal function of this protein. The predicted amino acid substitution is located in the cytoplasmic E1-E2 ATPase domain, suggesting that this variant may alter an important function of this protein. Assessment of this possibility can be achieved by analyzing tissues obtained from dogs with this variant. As noted earlier, however, human subjects with single amino acid substitutions at many dispersed locations in APT13A2 have similar progressive neurological disease, so it appears that most domains of the protein are important for its normal functioning.

The disease-related inclusion bodies that accumulated in neurological tissues were similar in both Tibetan Terriers and Australian Cattle Dogs with late-onset NCL. Membrane-bound autofluorescent inclusions (lipofuscin) also accumulate in many postmitotic cells during normal aging. However, the ultrastructural features of the disease-related inclusions were quite distinct from those of lipofuscin, both in nervous tissues and in the heart [14,49–61]. The disease-related inclusions in cardiac muscle of the affected dogs were quite unique and differed substantially from those in the brain and retina (Fig. 8). These inclusions consisted of a mixture of round bodies with contents that had either uniform electron density or a flocculent appearance. Based on their staining properties, uniformly stained bodies appear to be lipid droplets, whereas material within the bodies that co-localize with them appear to have carbohydrate moieties. Cardiac muscle pathology has not been studied extensively in the NCLs, so it would be of interest to determine whether similar inclusions accumulate in the hearts of people and dogs with all of the various forms of NCL. The disease-related storage material that accumulates in all cell types that were examined in the affected dogs were stained with an antibody that specifically labels the lysosomal marker protein LAMP1. Therefore, these cellular inclusions can be classified as lysosomal storage bodies.

Although only two littermate Australian Cattle Dogs and their mother have been identified that are homozygous for the mutant allele, a screen of 394 other Australian Cattle Dogs with no known close relationship to the affected dogs identified 42 dogs that were heterozygous for the variant, but no other homozygotes (Table 2). It is somewhat unexpected that with such a high carrier frequency, no dogs homozygous for the mutant allele were identified in the population sample. However, now that a fair number of heterozygotes have been identified, it should be possible to identify additional homozygous mutant dogs by selectively screening relatives of the carrier dogs for the mutant allele. Identification of additional affected dogs by such screening should open the possibility of obtaining tissues and cell lines to study ATP13A2 function, and in particular the function of the region of the protein modified by the p.(Thr373Ile) variant. Affected dogs identified by genetic screening may also serve as a model for preclinical therapeutic intervention studies for CLN12 disease. While the late onset of disease signs makes use of affected Australian Cattle Dogs impractical as a laboratory model for CLN12 disease, therapeutic studies could

be conducted by recruiting privately owned dogs for treatment studies. Such studies could provide preclinical data necessary for the conduct of human clinical trials for treatments for human CLN12 disease.

With respect to preventing the propagation of NCL in Australian Cattle Dogs, the relatively high incidence of the disease allele in the population tested indicates that it would be advisable to test dogs in the general population for the presence of this allele before using them for breeding. Because of the late onset of clinical signs, this is the only practical means by which to reduce the disease frequency in the breed. As would be expected, such screening for the disease alleles associated with a number of inherited diseases in purebred dogs has been effective in reducing the frequencies of these alleles and the associated diseases over time [62–66]. However, in cases where the frequency of the deleterious sequence variant is very high, it is important that maintaining genetic diversity within the breed be considered. In these cases, the best choice may be to continue to breed heterozygotes with dogs that are homozygous for the wildtype allele.

As with human CLN12 disease, relative to species lifespan the onset of clinical signs was later and the rate of disease progression slower in dogs with *ATP13A2*-related NCL than in most other forms of NCL [4]. Based on the known functions of the gene product in many of the other NCLs, the reason for the late onset of CLN12 disease is not clear, particularly since all of the known NCLs appear to result in impaired lysosomal function. The reason for this may become apparent with further study of the Australian Cattle Dog disease, particularly now that affected dogs can be identified by genetic screening prior to the onset of clinical signs. The relatively late onset of clinical signs in the canine and human forms of the disease means that with early detection via genetic screening there is a large time window during which therapeutic interventions may be undertaken that would prevent or delay disease onset and progression.

Supplementary Material

Refer to Web version on PubMed Central for supplementary material.

Acknowledgements

We thank all the owners who donated samples and information on their dogs. We also thank Eva Holderegger Walser for her help and communication with the owners and sample acquisition. Dr. Sabine Helmes provided blood samples and phenotype information from many dogs. Nathalie Besuchet Schmutz, Muriel Fragnière, Cheryl Jensen and Sabrina Schenk are gratefully acknowledged for expert technical assistance. The Next Generation Sequencing Platform and the Interfaculty Bioinformatics Unit of the University of Bern performed the whole genome sequencing experiment, and provided high performance computing infrastructure. We acknowledge collaborators of the Dog Biomedical Variant Database Consortium (DBVDC), Gus Aguirre, Catherine André, Danika Bannasch, Doreen Becker, Brian Davis, Cord Drögemüller, Kari Ekenstedt, Kiterie Faller, Oliver Forman, Steve Friedenbergh, Eva Furrow, Urs Giger, Christophe Hitte, Marjo Hytönen, Hannes Lohi, Cathryn Mellersh, Jim Mickelson, Leonardo Murgiano, Anita Oberbauer, Sheila Schmutz, Jeffrey Schoenebeck, Kim Summers, Frank van Steenbeek, Claire Wade for sharing whole genome sequence data from control dogs and wolves. We also acknowledge all canine researchers who deposited dog whole genome sequencing data into public databases. This study was supported in part by a grant from the Albert-Heim Foundation (no. 105) and grant EY023968 from the U.S. National Institutes of Health.

References

- [1]. Mole SE, Williams RE, Goebel HH, The Neuronal Ceroid Lipofuscinoses (Batten Disease), Oxford University Press, Great Britain, Oxford, 2011.
- [2]. Warriar V, Vieira M, Mole SE, Genetic basis and phenotypic correlations of the neuronal ceroid lipofuscinoses, *Biochim. Biophys. Acta* 1832 (2013) 1827–1830. [PubMed: 23542453]
- [3]. Kousi M, Lehesjoki AE, Mole SE, Update of the mutation spectrum and clinical correlations of over 360 mutations in eight genes that underlie the neuronal ceroid lipofuscinoses, *Hum. Mutat* 33 (2012) 42–63. [PubMed: 21990111]
- [4]. Katz ML, Rustad E, Robinson GO, Whiting REH, Student JT, Coates JR, Narfstrom K, Canine neuronal ceroid lipofuscinoses: promising models for pre-clinical testing of therapeutic interventions, *Neurobiol. Dis* 108 (2017) 277–287. [PubMed: 28860089]
- [5]. Lingaas F, Guttersrud OA, Arnet E, Espenes A, Neuronal ceroid lipofuscinosis in salukis is caused by a single base pair insertion in CLN8, *Anim. Genet* 49 (2018) 52–58. [PubMed: 29446145]
- [6]. Kolicheski A, Johnson GS, O'Brien DP, Mhlanga-Mutangadura T, Gilliam D, Guo J, Anderson-Sieg TD, Schnabel RD, Taylor JF, Lebowitz A, Swanson B, Hicks D, Niman ZE, Wininger FA, Carpentier MC, Katz ML, Australian cattle dogs with neuronal Ceroid Lipofuscinosis are homozygous for a CLN5 nonsense mutation previously identified in border collies, *J. Vet. Intern. Med* 30 (2016) 1149–1158. [PubMed: 27203721]
- [7]. Melville SA, Wilson CL, Chiang CS, Studdert VP, Lingaas F, Wilton AN, A mutation in canine CLN5 causes neuronal ceroid lipofuscinosis in Border collie dogs, *Genomics* 86 (2005) 287–294. [PubMed: 16033706]
- [8]. Katz ML, Coates JR, Cooper JJ, O'Brien DP, Jeong M, Narfstrom K, Retinal pathology in a canine model of late infantile neuronal ceroid lipofuscinosis, *Invest. Ophthalmol. Vis. Sci* 49 (2008) 2686–2695. [PubMed: 18344450]
- [9]. Morgan BR, Coates JR, Johnson GC, Shelton GD, Katz ML, Characterization of thoracic motor and sensory neurons and spinal nerve roots in canine degenerative myelopathy, a potential disease model of amyotrophic lateral sclerosis, *J. Neurosci. Res* 92 (2014) 531–541. [PubMed: 24375814]
- [10]. Katz ML, Redmond TM, Effect of Rpe65 knockout on accumulation of lipofuscin fluorophores in the retinal pigment epithelium, *Invest. Ophthalmol. Vis. Sci* 42 (2001) 3023–3030. [PubMed: 11687551]
- [11]. Estrada-Cuzcano A, Martin S, Chamova T, Synofzik M, Timmann D, Hølemans T, Andreeva A, Reichbauer J, De Rycke R, Chang DI, van Veen S, Samuel J, Schols L, Poppel T, Møllerup Sørensen D, Asselbergh B, Klein C, Zuchner S, Jordanova A, Vangheluwe P, Tournev I, Schule R, Loss-of-function mutations in the ATP13A2/PARK9 gene cause complicated hereditary spastic paraplegia (SPG78), *Brain* 140 (2017) 287–305. [PubMed: 28137957]
- [12]. Cingolani P, Platts A, Wang IL, Coon M, Nguyen T, Wang L, Land SJ, Lu X, Ruden DM, A program for annotating and predicting the effects of single nucleotide polymorphisms, SnpEff: SNPs in the genome of *Drosophila melanogaster* strain w1118; iso-2; iso-3, *Fly* 6 (2012) 80–92. [PubMed: 22728672]
- [13]. Bai B, Zhao WM, Tang BX, Wang YQ, Wang L, Zhang Z, Yang HC, Liu YH, Zhu JW, Irwin DM, Wang GD, Zhang YP, DoGSD: the dog and wolf genome SNP database, *Nucleic Acids Res.* 43 (2015) D777–D783. [PubMed: 25404132]
- [14]. Fawcett DW, The Cell WB Saunders, Philadelphia, 1981.
- [15]. Jolly RD, Palmer DN, The neuronal ceroid-lipofuscinoses (batten disease): comparative aspects, *Neuropathol. Appl. Neurobiol* 21 (1995) 50–60.
- [16]. Jolly RD, Dalefield RR, Palmer DN, Ceroid, lipofuscin and the ceroid-lipofuscinoses (batten disease), *J. Inherit. Metab. Dis* 16 (1993) 280–283.
- [17]. Jolly RD, Martinus RD, Palmer DN, Sheep and other animals with ceroid-lipofuscinoses: their relevance to batten disease, *Am. J. Med. Genet* 42 (1992) 609–614. [PubMed: 1535180]
- [18]. Kolicheski A, Barnes Heller HL, Arnold S, Schnabel RD, Taylor JF, Knox CA, Mhlanga-Mutangadura T, O'Brien DP, Johnson GS, Dreyfus J, Katz ML, Homozygous PPT1 splice donor

- mutation in a cane Corso dog with neuronal ceroid lipofuscinosis, *J. Vet. Intern. Med* 31 (2017) 149–157. [PubMed: 28008682]
- [19]. Ashwini A, D'Angelo A, Yamato O, Giordano C, Cagnotti G, Harcourt-Brown T, Mhlanga-Mutangadura T, Guo J, Johnson GS, Katz ML, Neuronal ceroid lipofuscinosis associated with an MFSD8 mutation in Chihuahuas, *Mol. Genet. Metab* 118 (2016) 326–332. [PubMed: 27211611]
- [20]. Bruun I, Reske-Nielsen E, Oster S, Juvenile ceroid-lipofuscinosis and calcifications of the CNS *Acta Neurol Scand* 83 (1991) 1–8. [PubMed: 2011942]
- [21]. Tyynela J, Cooper JD, Khan MN, Shemilts SJ, Haltia M, Hippocampal Pathology in the Human Neuronal Ceroid-Lipofuscinoses: Distinct Patterns of Storage Deposition, Neurodegeneration and Glial Activation Brain Pathology, vol. 14, (2004), pp. 349–357. [PubMed: 15605981]
- [22]. Najim al-Din AS, Wriekat A, Mubaidin A, Dasouki M, Hiari M, Pallido-pyramidal degeneration, supranuclear upgaze paresis and dementia: Kufor-Rakeb syndrome, *Acta Neurol. Scand* 89 (1994) 347–352. [PubMed: 8085432]
- [23]. Ramirez A, Heimbach A, Grundemann J, Stiller B, Hampshire D, Cid LP, Goebel I, Mubaidin AF, Wriekat AL, Roeper J, Al-Din A, Hillmer AM, Karsak M, Liss B, Woods CG, Behrens MI, Kubisch C, Hereditary parkinsonism with dementia is caused by mutations in ATP13A2, encoding a lysosomal type 5 P-type ATPase, *Nat. Genet* 38 (2006) 1184–1191. [PubMed: 16964263]
- [24]. Behrens MI, Bruggemann N, Chana P, Venegas P, Kagi M, Parrao T, Orellana P, Garrido C, Rojas CV, Hauke J, Hahnen E, Gonzalez R, Seleme N, Fernandez V, Schmidt A, Binkofski F, Kompf D, Kubisch C, Hagenah J, Klein C, Ramirez A, Clinical spectrum of Kufor-Rakeb syndrome in the Chilean kindred with ATP13A2 mutations, *Mov. Disord* 25 (2010) 1929–1937. [PubMed: 20683840]
- [25]. Bruggemann N, Hagenah J, Reetz K, Schmidt A, Kasten M, Buchmann I, Eckerle S, Bahre M, Munchau A, Djarmati A, van der Vejt J, Siebner H, Binkofski F, Ramirez A, Behrens MI, Klein C, Recessively inherited parkinsonism: effect of ATP13A2 mutations on the clinical and neuroimaging phenotype, *Arch. Neurol* 67 (2010) 1357–1363. [PubMed: 21060012]
- [26]. Di Fonzo A, Chien HF, Socal M, Giraudo S, Tassorelli C, Iliceto G, Fabbrini G, Marconi R, Fincati E, Abbruzzese G, Marini P, Squitieri F, Horstink MW, Montagna P, Libera AD, Stocchi F, Goldwurm S, Ferreira JJ, Meco G, Martignoni E, Lopiano L, Jardim LB, Oostra BA, Barbosa ER, Italian Parkinson Genetics N, Bonifati V, ATP13A2 missense mutations in juvenile parkinsonism and young onset Parkinson disease, *Neurology* 68 (2007) 1557–1562. [PubMed: 17485642]
- [27]. Eiberg H, Hansen L, Korbo L, Nielsen IM, Svenstrup K, Bech S, Pinborg LH, Friberg L, Hjerminde LE, Olsen OR, Nielsen JE, Novel mutation in ATP13A2 widens the spectrum of Kufor-Rakeb syndrome (PARK9), *Clin. Genet* 82 (2012) 256–263. [PubMed: 21696388]
- [28]. Martino D, Melzi V, Franco G, Kandasamy N, Monfrini E, Di Fonzo A, Juvenile dystonia-parkinsonism syndrome caused by a novel p.S941Tfs1X ATP13A2 (PARK9) mutation, *Parkinsonism Relat. Disord* 21 (2015) 1378–1380. [PubMed: 26421390]
- [29]. Park JS, Blair NF, Sue CM, The role of ATP13A2 in Parkinson's disease: clinical phenotypes and molecular mechanisms, *Mov. Disord* 30 (2015) 770–779. [PubMed: 25900096]
- [30]. Park JS, Mehta P, Cooper AA, Veivers D, Heimbach A, Stiller B, Kubisch C, Fung VS, Krainc D, Mackay-Sim A, Sue CM, Pathogenic effects of novel mutations in the P-type ATPase ATP13A2 (PARK9) causing Kufor-Rakeb syndrome, a form of early-onset parkinsonism, *Hum. Mutat* 32 (2011) 956–964. [PubMed: 21542062]
- [31]. Park JS, Sue CM, Hereditary parkinsonism-associated genetic variations in PARK9 locus Lead to functional impairment of ATPase type 13A2, *Curr. Protein Pept. Sci* 18 (2017) 725–732. [PubMed: 26965689]
- [32]. Yang X, Xu Y, Mutations in the ATP13A2 gene and parkinsonism: a preliminary review, *Biomed. Res. Int* 2014 (2014) 371256. [PubMed: 25197640]
- [33]. Kara E, Tucci A, Manzoni C, Lynch DS, Elpidorou M, Bettencourt C, Chelban V, Manole A, Hamed SA, Haridy NA, Federoff M, Preza E, Hughes D, Pittman A, Jaunmuktane Z, Brandner S, Xiromerisiou G, Wiethoff S, Schottlaender L, Proukakis C, Morris H, Warner T, Bhatia KP, Korlipara LV, Singleton AB, Hardy J, Wood NW, Lewis PA, Houlden H, Genetic and phenotypic characterization of complex hereditary spastic paraplegia, *Brain* 139 (2016) 1904–1918. [PubMed: 27217339]

- [34]. Grunewald A, Arns B, Seibler P, Rakovic A, Munchau A, Ramirez A, Sue CM, Klein C, ATP13A2 mutations impair mitochondrial function in fibroblasts from patients with Kufor-Rakeb syndrome, *Neurobiol. Aging* 33 (2012) 1843.e1841–1847.
- [35]. Gusdon AM, Zhu J, Van Houten B, Chu CT, ATP13A2 regulates mitochondrial bioenergetics through macroautophagy, *Neurobiol. Dis* 45 (2012) 962–972. [PubMed: 22198378]
- [36]. Park JS, Koentjoro B, Veivers D, Mackay-Sim A, Sue CM, Parkinson's disease-associated human ATP13A2 (PARK9) deficiency causes zinc dyshomeostasis and mitochondrial dysfunction, *Hum. Mol. Genet* 23 (2014) 2802–2815. [PubMed: 24399444]
- [37]. Dehay B, Martinez-Vicente M, Ramirez A, Perier C, Klein C, Vila M, Bezdard E, Lysosomal dysfunction in Parkinson disease: ATP13A2 gets into the groove, *Autophagy* 8 (2012) 1389–1391. [PubMed: 22885599]
- [38]. Holemans T, Sorensen DM, van Veen S, Martin S, Hermans D, Kemmer GC, Van den Haute C, Baekelandt V, Gunther Pomorski T, Agostinis P, Wuytack F, Palmgren M, Eggermont J, Vangheluwe P, A lipid switch unlocks Parkinson's disease-associated ATP13A2, *Proc. Natl. Acad. Sci. U. S. A* 112 (2015) 9040–9045. [PubMed: 26134396]
- [39]. Kong SM, Chan BK, Park JS, Hill KJ, Aitken JB, Cottle L, Farghaian H, Cole AR, Lay PA, Sue CM, Cooper AA, Parkinson's disease-linked human PARK9/ATP13A2 maintains zinc homeostasis and promotes alpha-Synuclein externalization via exosomes, *Hum. Mol. Genet* 23 (2014) 2816–2833. [PubMed: 24603074]
- [40]. Sato S, Koike M, Funayama M, Ezaki J, Fukuda T, Ueno T, Uchiyama Y, Hattori N, Lysosomal storage of subunit c of mitochondrial ATP synthase in brain-specific Atp13a2-deficient mice, *Am. J. Pathol* 186 (2016) 3074–3082. [PubMed: 27770614]
- [41]. Kett LR, Stiller B, Bernath MM, Tasset I, Blesa J, Jackson-Lewis V, Chan RB, Zhou B, Di Paolo G, Przedborski S, Cuervo AM, Dauer WT, Alpha-Synuclein-independent histopathological and motor deficits in mice lacking the endolysosomal parkinsonism protein Atp13a2, *J. Neurosci* 35 (2015) 5724–5742. [PubMed: 25855184]
- [42]. Matsui H, Sato F, Sato S, Koike M, Taruno Y, Saiki S, Funayama M, Ito H, Taniguchi Y, Uemura N, Toyoda A, Sakaki Y, Takeda S, Uchiyama Y, Hattori N, Takahashi R, ATP13A2 deficiency induces a decrease in cathepsin D activity, fingerprint-like inclusion body formation, and selective degeneration of dopaminergic neurons, *FEBS Lett* 587 (2013) 1316–1325. [PubMed: 23499937]
- [43]. Demirsoy S, Martin S, Motamedi S, van Veen S, Holemans T, Van den Haute C, Jordanova A, Baekelandt V, Vangheluwe P, Agostinis P, ATP13A2/PARK9 regulates endo-/lysosomal cargo sorting and proteostasis through a novel PI(3, 5)P2-mediated scaffolding function, *Hum. Mol. Genet* 26 (2017) 1656–1669. [PubMed: 28334751]
- [44]. Bento CF, Ashkenazi A, Jimenez-Sanchez M, Rubinsztein DC, The Parkinson's disease-associated genes ATP13A2 and SYT11 regulate autophagy via a common pathway, *Nat. Commun* 7 (2016) 11803. [PubMed: 27278822]
- [45]. Farias FH, Zeng R, Johnson GS, Wininger FA, Taylor JF, Schnabel RD, McKay SD, Sanders DN, Lohi H, Seppala EH, Wade CM, Lindblad-Toh K, O'Brien DP, Katz ML, A truncating mutation in ATP13A2 is responsible for adult-onset neuronal ceroid lipofuscinosis in Tibetan terriers, *Neurobiol. Dis* 42 (2011) 468–474. [PubMed: 21362476]
- [46]. Wohlke A, Philipp U, Bock P, Beineke A, Lichtner P, Meitinger T, Distl O, A one base pair deletion in the canine ATP13A2 gene causes exon skipping and late-onset neuronal ceroid lipofuscinosis in the Tibetan terrier, *PLoS Genet*. 7 (2011) e1002304. [PubMed: 22022275]
- [47]. Bras J, Verloes A, Schneider SA, Mole SE, Guerreiro RJ, Mutation of the parkinsonism gene ATP13A2 causes neuronal ceroid-lipofuscinosis, *Hum. Mol. Genet* 21 (2012) 2646–2650. [PubMed: 22388936]
- [48]. Katz ML, Narfstrom K, Johnson GS, O'Brien DP, Assessment of retinal function and characterization of lysosomal storage body accumulation in the retinas and brains of Tibetan terriers with ceroid-lipofuscinosis, *Am. J. Vet. Res* 66 (2005) 67–76. [PubMed: 15691038]
- [49]. Armstrong D, Free radical involvement in the formation of lipopigments, in: Armstrong D, Sohal RS, Cutler RG, Slater TF (Eds.), *Free Radicals in Molecular Biology, Aging, and Disease*, Raven Press, New York, 1984, pp. 129–141.

- [50]. Hashemzadeh-Bonehi L, Phillips RG, Cairns NJ, Mosaheb S, Thorpe JR, Pin1 protein associates with neuronal lipofuscin: potential consequences in age-related neurodegeneration, *Exp. Neurol* 199 (2006) 328–338. [PubMed: 16480979]
- [51]. Jasty V, Jamison JR, Hartnagel RE, Three types of cytoplasmic granules in cardiac muscle cells of cynomolgus monkeys (*Macaca fascicularis*), *Vet. Pathol* 21 (1984) 505–508. [PubMed: 6207657]
- [52]. Jolly RD, Douglas BV, Davey PM, Roiri JE, Lipofuscin in bovine muscle and brain: a model for studying age pigment *Gerontology* 41 Suppl 2 (1995) 283–295.
- [53]. Jung H, Lee EY, Lee SI, Age-related changes in ultrastructural features of cathepsin B- and D-containing neurons in rat cerebral cortex, *Brain Res.* 844 (1999) 43–54. [PubMed: 10536260]
- [54]. Koobs DH, Schultz RL, Jutzy RV, The Origin of Lipofuscin and Possible Consequences to the Myocardium *Archives of Pathology & Laboratory Medicine*, vol. 102, (1978), pp. 66–68. [PubMed: 579966]
- [55]. Riis RC, Cummings JF, Loew ER, de Lahunta A, Tibetan terrier model of canine ceroid lipofuscinosis, *Am. J. Med. Genet* 42 (1992) 615–621. [PubMed: 1609844]
- [56]. Sandusky GE Jr., C.C. Capen, K.M. Kerr, Histological and ultrastructural evaluation of cardiac lesions in idiopathic cardiomyopathy in dogs, *Canadian Journal of Comparative Medicine* 48 (1984) 81–86. [PubMed: 6713261]
- [57]. Siakotos AN, Koppang N, Procedures for the isolation of lipopigments from brain, heart and liver, and their properties: a review, *Mech. Ageing Dev* 2 (1973) 177–200. [PubMed: 4584835]
- [58]. Siakotos AN, Watanabe I, Saito A, Fleischer S, Procedures for the isolation of two distinct lipopigments from human brain: lipofuscin and ceroid, *Biochemical Medicine* 4 (1970) 361–375. [PubMed: 4332499]
- [59]. Sohal RS, Wolfe LS, Lipofuscin: characteristics and significance, *Prog. Brain Res* 70 (1986) 171–183. [PubMed: 3554350]
- [60]. Sulzer D, Mosharov E, Tallozy Z, Zucca FA, Simon JD, Zecca L, Neuronal pigmented autophagic vacuoles: lipofuscin, neuromelanin, and ceroid as macro-autophagic responses during aging and disease, *J. Neurochem* 106 (2008) 24–36. [PubMed: 18384642]
- [61]. Tripathi S, Mahdi AA, Nawab A, Chander R, Hasan M, Siddiqui MS, Mahdi F, Mitra K, Bajpai VK, Influence of age on aluminum induced lipid peroxidation and neurolipofuscin in frontal cortex of rat brain: a behavioral, biochemical and ultra-structural study, *Brain Res.* 1253 (2009) 107–116. [PubMed: 19073157]
- [62]. Jolly RD, Dodds WJ, Ruth GR, Trauner DB, Screening for genetic diseases: principles and practice, *Adv. Vet. Sci. Comp. Med* 25 (1981) 245–276. [PubMed: 7034500]
- [63]. Mellersh C, DNA testing and domestic dogs, *Mamm. Genome* 23 (2012) 109–123. [PubMed: 22071879]
- [64]. Metallinos DL, Canine molecular genetic testing, *Vet. Clin. North Am. Small Anim. Pract* 31 (2001) 421–431. [PubMed: 11265501]
- [65]. Traas AM, Casal M, Haskins M, Henthorn P, Genetic counseling in the era of molecular diagnostics, *Theriogenology* 66 (2006) 599–605. [PubMed: 16777204]
- [66]. Kluth S, Eckardt J, Distl O, Selection response to DNA testing for canine ceroid lipofuscinosis in Tibetan terriers, *Vet. J* 201 (2014) 433–434. [PubMed: 24929534]

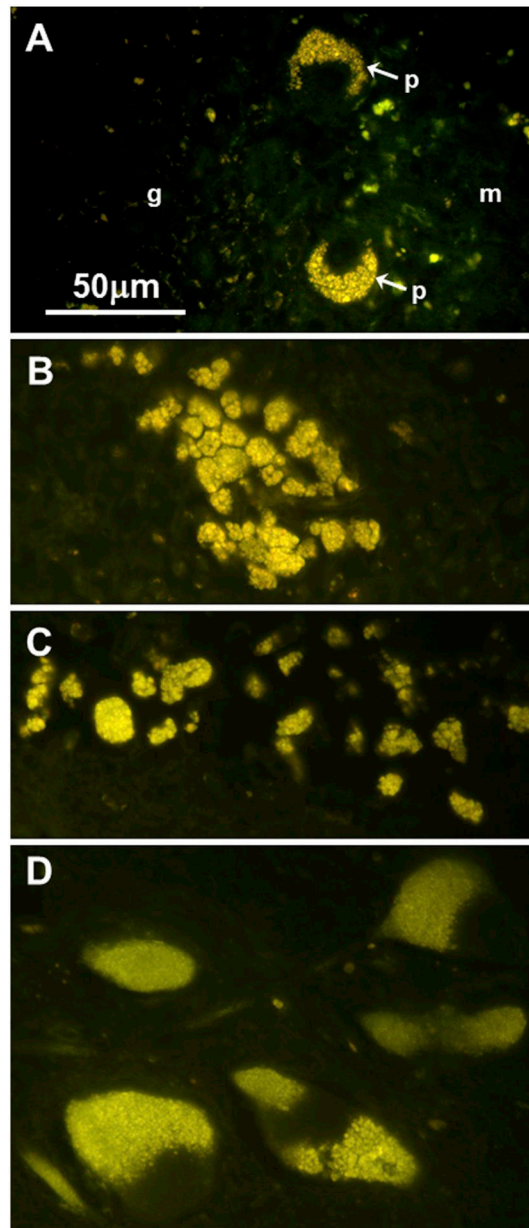


Fig. 1. Fluorescence micrographs unstained sections of the cerebellar Purkinje cell layer (A and B), the cerebellar meninges (C), and a deep cerebellar nucleus (D) from dog C. Massive accumulations of yellow-emitting autofluorescent material was present primarily in these areas of the cerebellum. Bar in (A) indicates the magnification of a 4 micrographs. In (A) p= Purkinje cell; m= molecular layer; g= granule cell layer. (For interpretation of the references to colour in this figure legend, the reader is referred to the web version of this article.)

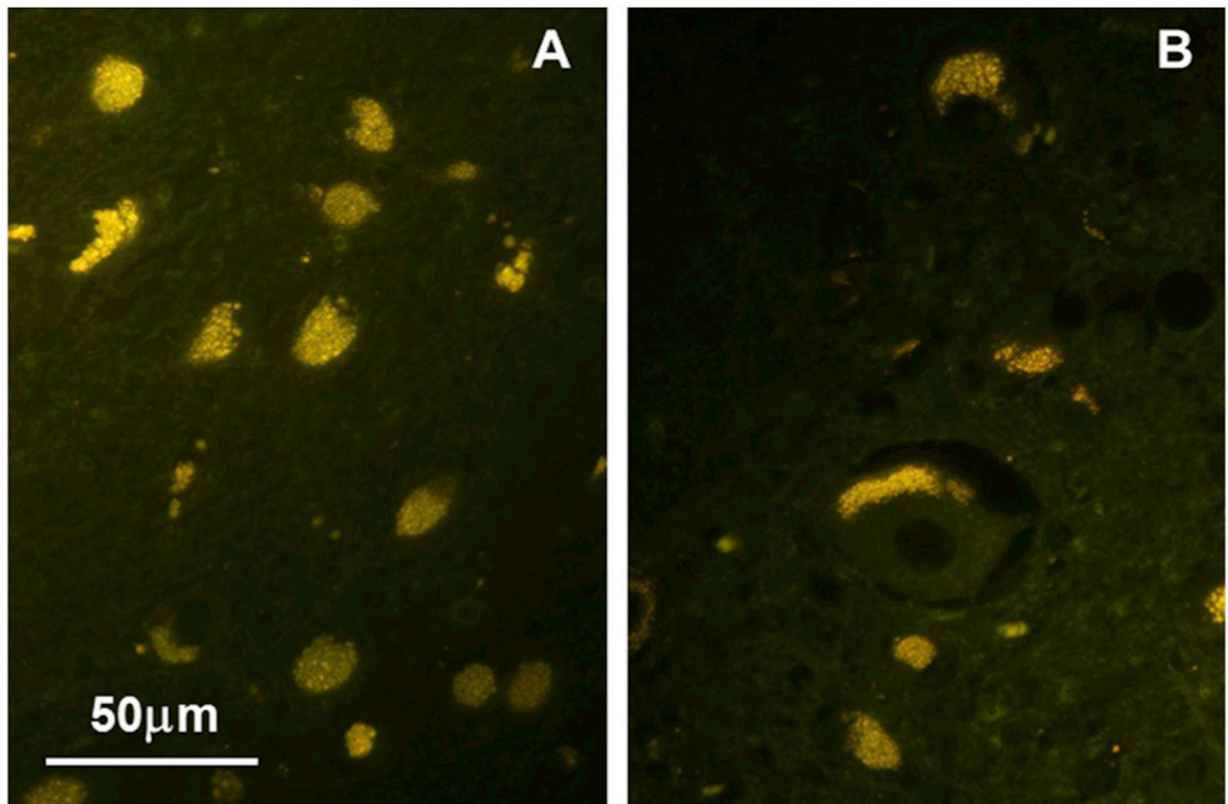


Fig. 2. Fluorescence micrographs of unstained sections of the parietal cerebral cortex of dog B. Autofluorescent storage material was present in almost all of the cerebral cortical neurons, and in the larger neurons could be seen to be localized within the perinuclear region of the cells (B). Bar in (B) indicates the magnification of both micrographs.

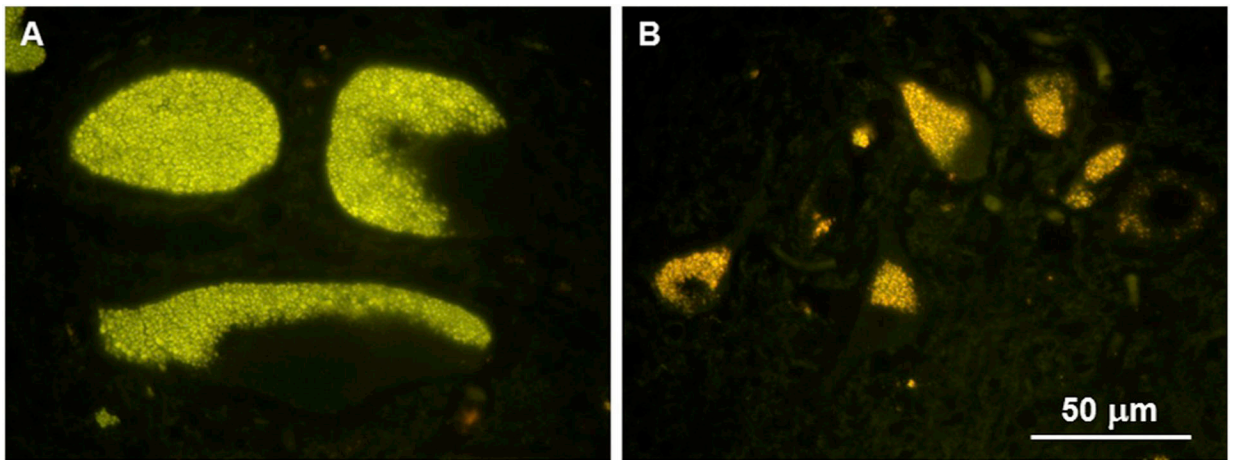


Fig. 3. Fluorescence micrographs of the ventral (A) and dorsal (B) horns of an unstained section of cervical spinal cord from dog C showing massive accumulations of autofluorescent storage material in neurons throughout the spinal cord gray matter. Bar in (B) indicates the magnification of both micrographs.

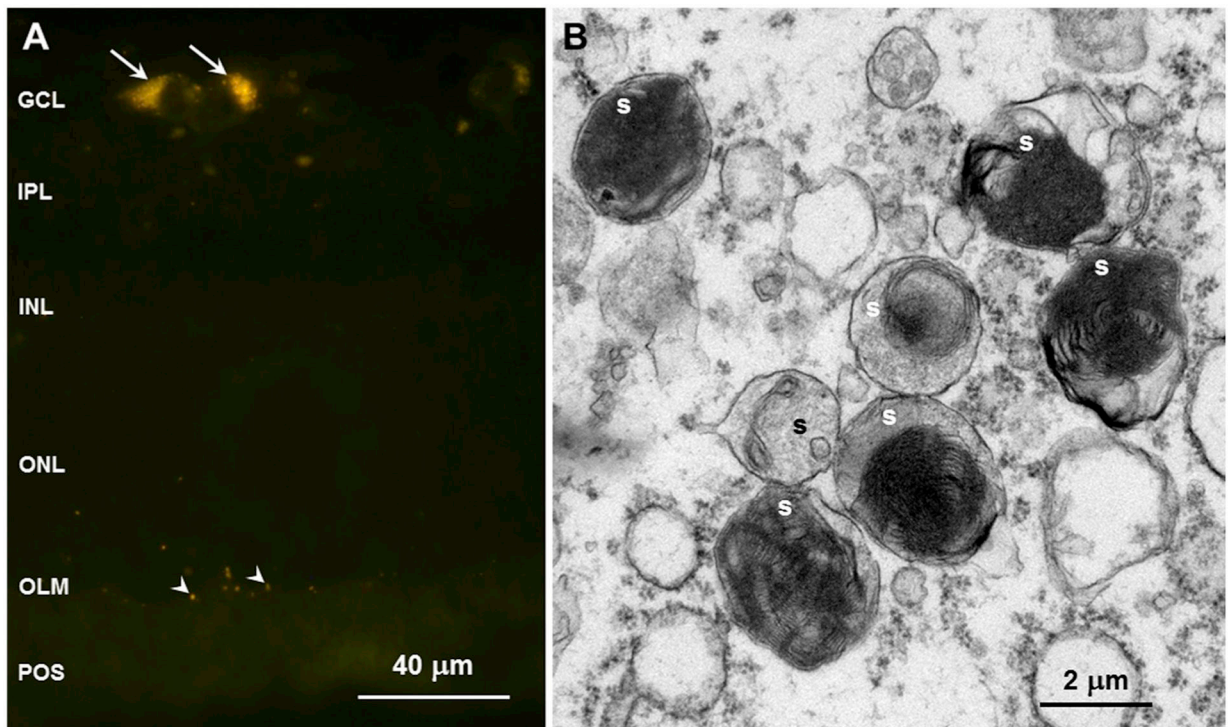


Fig. 4.

(A) Fluorescence micrograph of un-stained section of the retina from dog C.

Autofluorescent material was present in the cell bodies of the ganglion cells (arrows) and small punctate autofluorescent bodies were present along the outer limiting membrane (olm). (B) Electron micrograph of disease-sepdific storage bodies (s) in a retinal ganglion cell from dog C. Abbreviations: GCL, ganglion cell layer; IPL, inner plexiform layer; INL, inner nuclear layer; ONL, outer nuclear layer; OLM, outer limiting memberane; POS, photoreceptor outer segments.

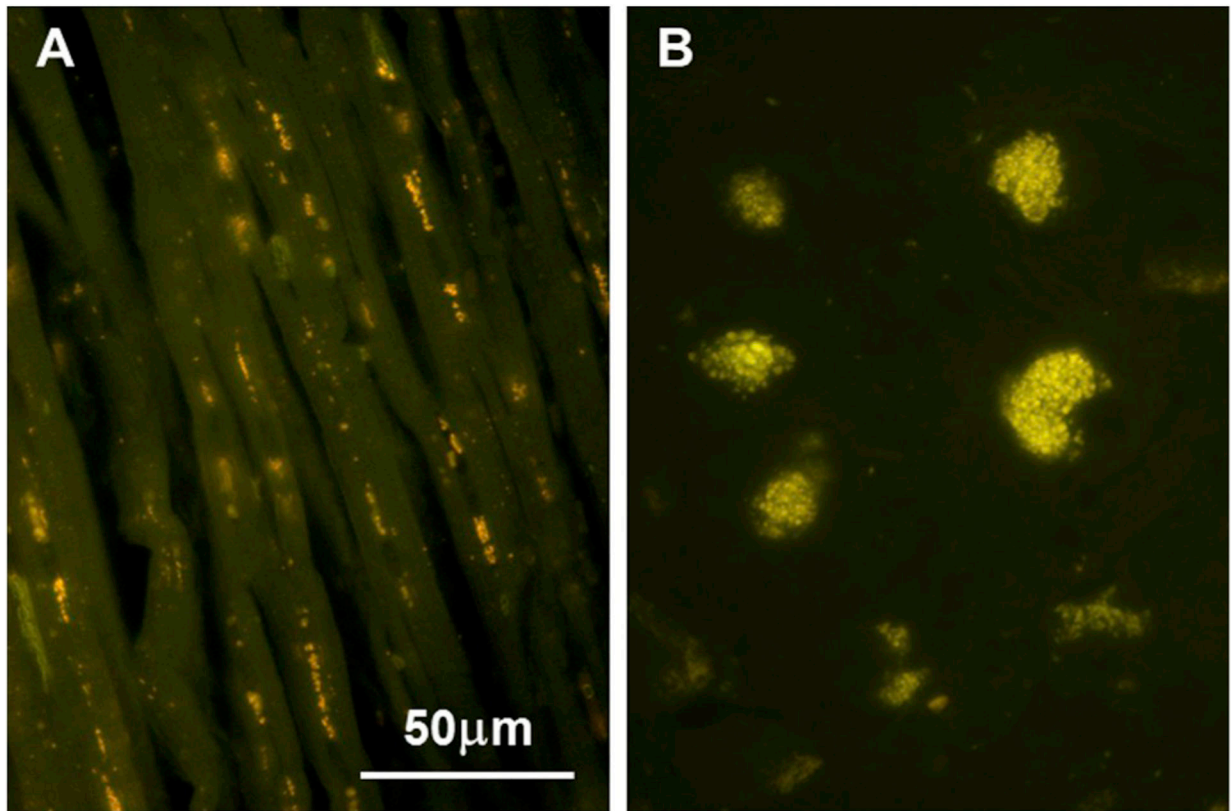


Fig. 5. Fluorescence micrographs of sections of cardiac ventricular wall from affected dog B. Strands of autofluorescent granules were present along the cardiac muscle fibers arranged parallel with the longitudinal orientation of muscle fibers (A). Aggregates of autofluorescent inclusions were also present in neurons of cardiac ganglia (B). Bar in (A) indicates the magnification of both micrographs.

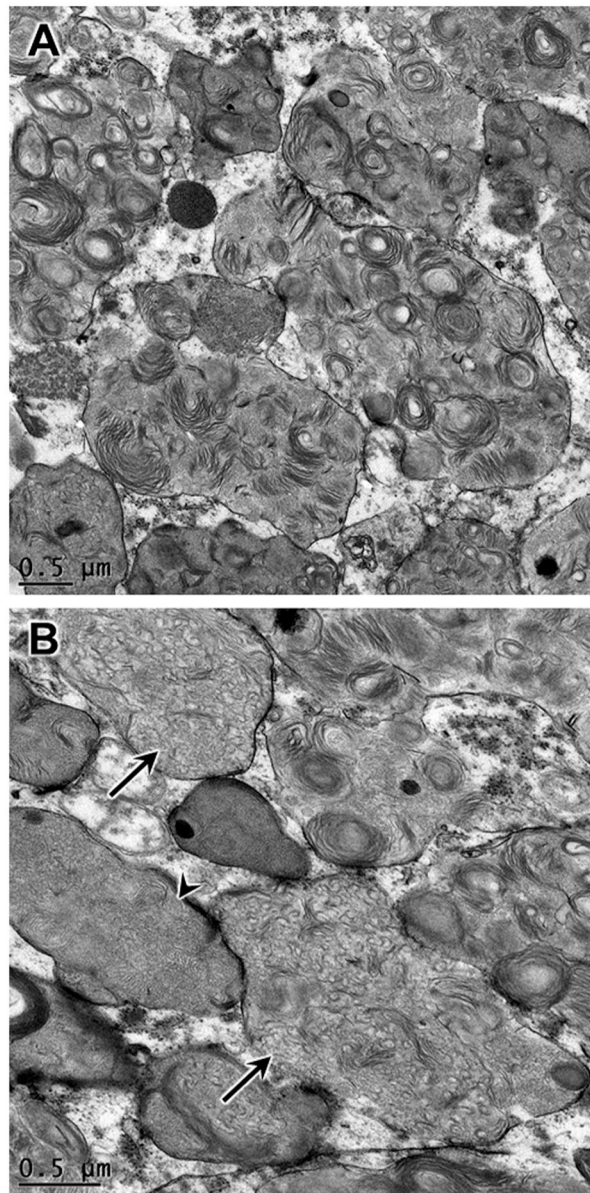


Fig. 6. Electron micrographs of disease-related inclusion bodies in the cerebellar Purkinje layer from affected dog B. Individual membrane-bound inclusions occurred in tightly-packed clusters. The contents of the majority of the inclusion bodies consisted of whorls and stacks of membrane-like structures (A), but the contents of some inclusionbodies consisted primarily of curvilinear structures (arrows in B) or of tightly-packed fine membrane-like material (arrowhead inB).

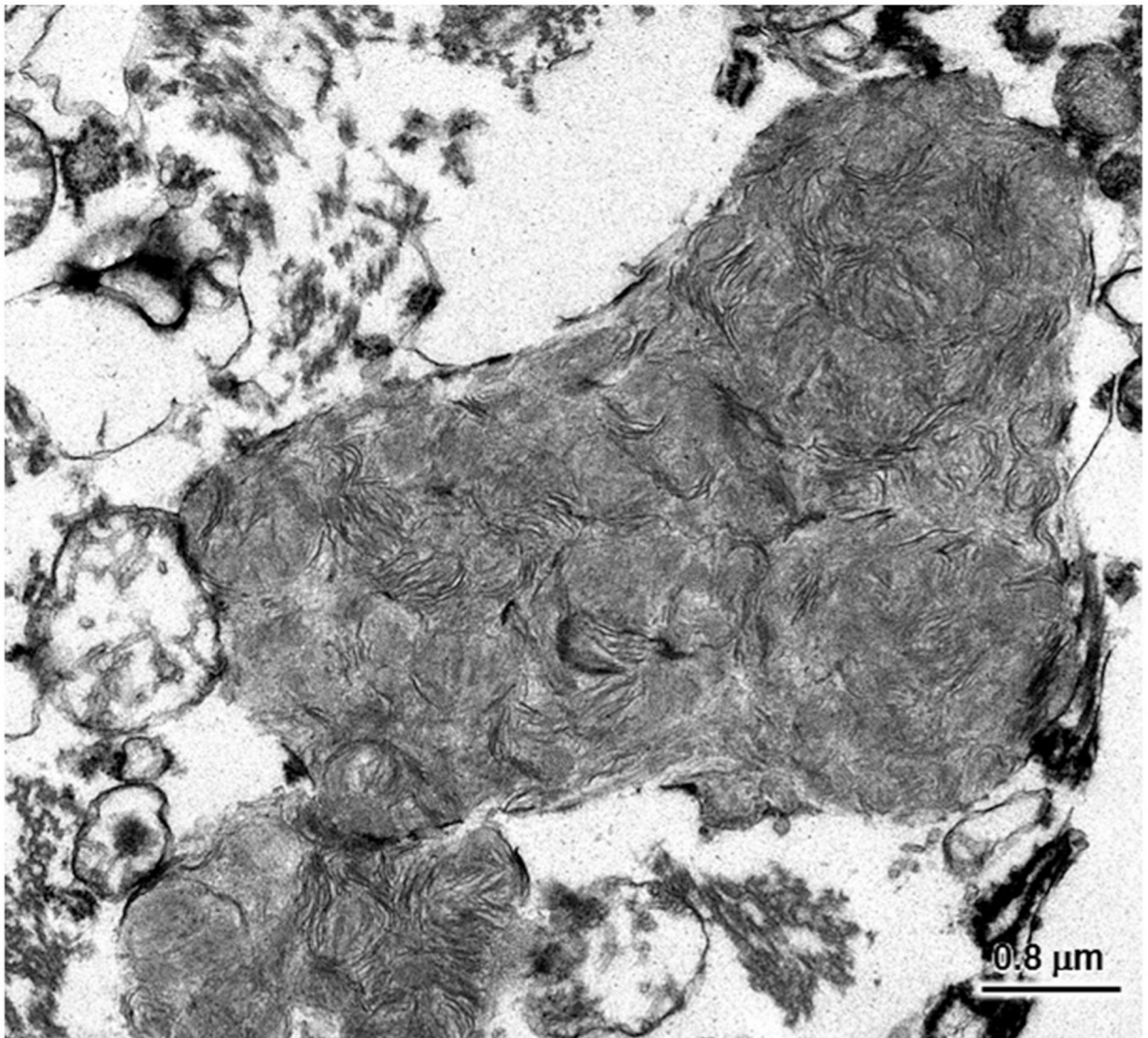


Fig. 7.
Electron micrograph showing disease-related inclusion in a neuron from the parietal cerebral cortex of affected dog C.

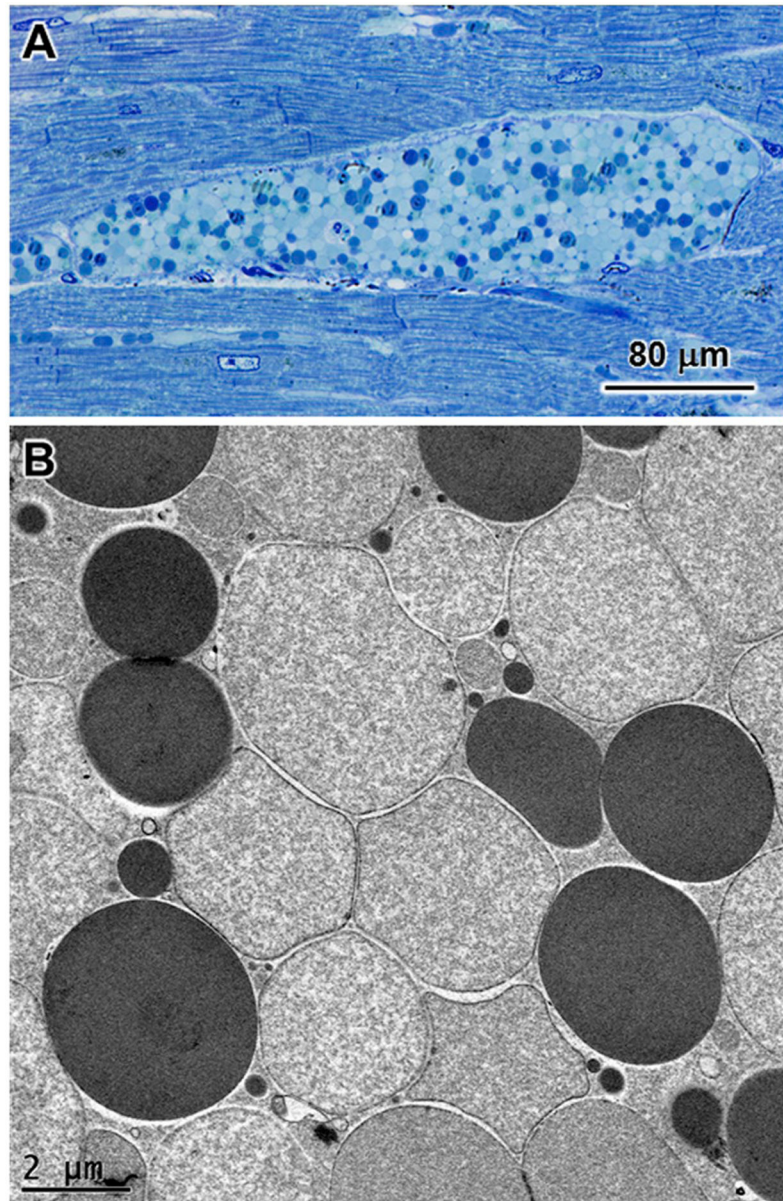


Fig. 8. (A) Light micrograph of a large cluster of inclusion bodies in the cardiac muscle the heart ventricle of affected dog B. (B) Electron micrograph of the same type of inclusion bodies in cells adjacent to the cardiac muscle fibers of affected dog B.

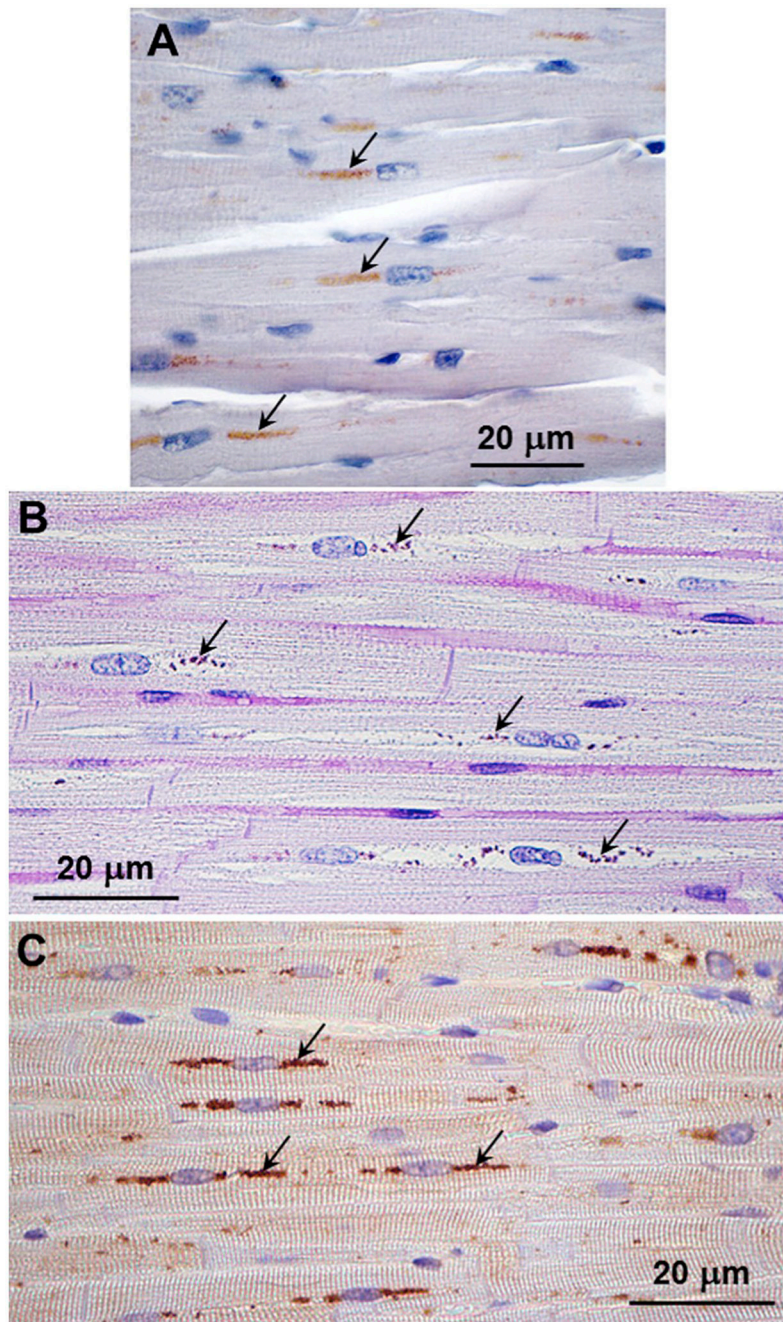


Fig. 9. Light micrographs of sections of heart ventricle cardiac muscles from an affected dog stained with Sudan black III (A), periodic acid Schiff reagent (B), and immunostained with an anti-LAMP1 antibody. Arrows indicate disease-related inclusion bodies.

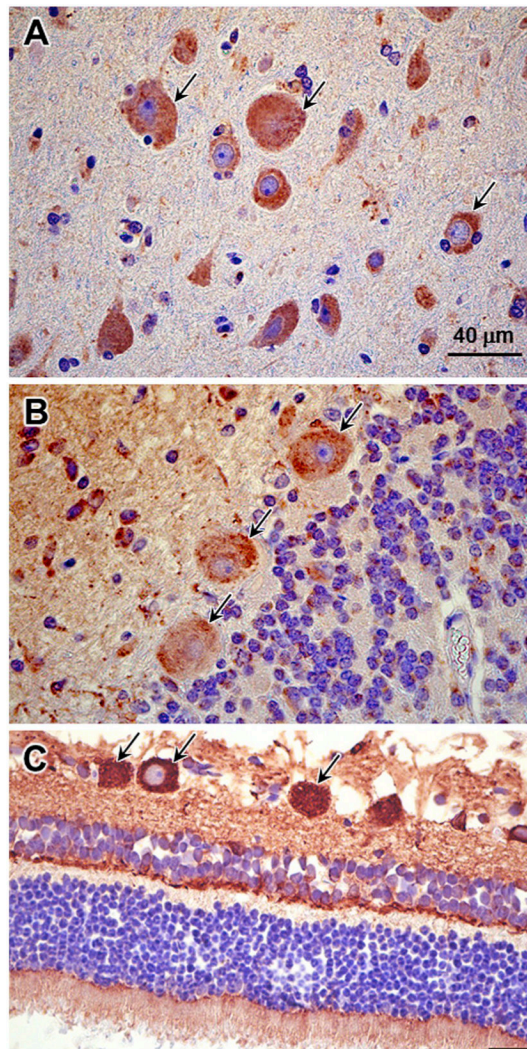


Fig. 10. Light micrographs of paraffin sections of cerebral cortex (A), cerebellum(B) and retina (C) from an affected dog. Sections were immunostained with an antibody against the lysosomal marker LAMP1. Inclusion bodies in cerebral cortical neurons (arrows in A), cerebellar Purkinje cells (arrows in B), and retinal ganglion cells (arrows in C) stained with the anti-LAMP1 antibody. Bar in B indicates magnification of all 3 micrographs.

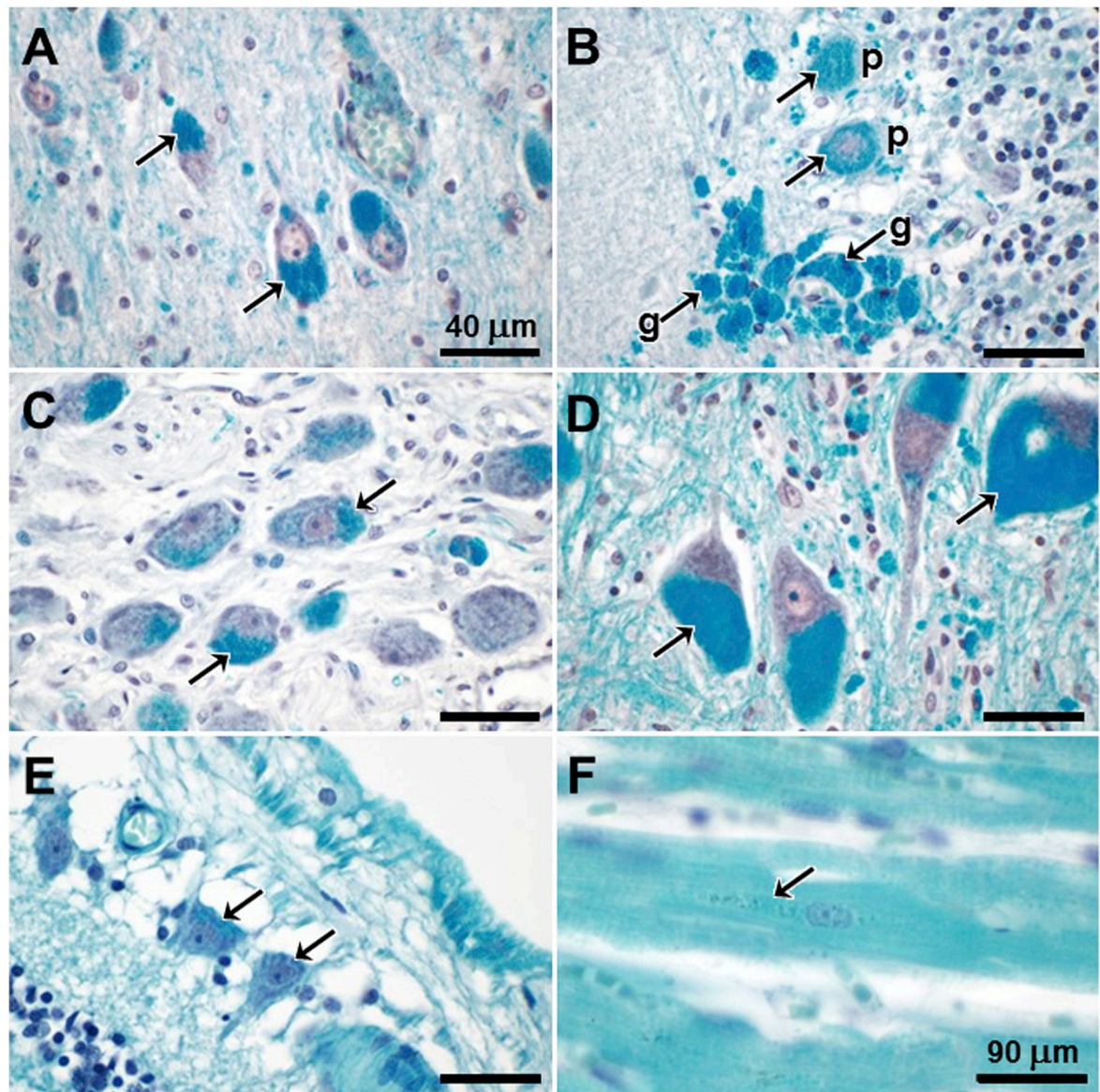


Fig. 11.

Luxol fast blue stained paraffin sections of cerebral cortex (A), cerebellar cortex (B), ciliary ganglion (C), thalamus (D), retina (E), and cardiac muscle. Arrows indicate specific Luxol fast blue staining. In panel (B) the staining is apparent in both the Purkinje cells (p) and the large non-Purkinje cell aggregates in the Purkinje cell layer (g). In panel (E) the stained cells indicated by arrows are retinal ganglion cells. In the cardiac muscle the specific staining could be seen despite relatively high background staining in this tissue. In all cases, the localization of the stained inclusions was the same as the autofluorescence in unstained sections. Bar in (A) indicates the magnification of panels (A-E). (For interpretation of the references to colour in this figure legend, the reader is referred to the web version of this article.)

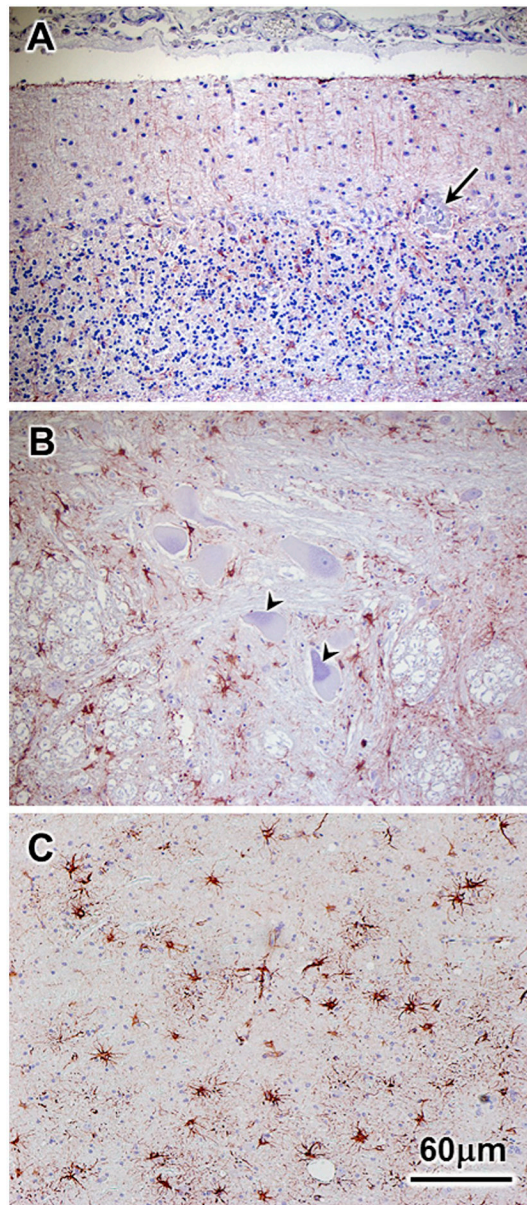


Fig. 12. GFAP IHC stained sections of cerebellar cortex (A), a deep cerebellar nucleus (B), and the parietal cerebral cortex from affected dog C. No significant astrogliosis was observed in the cerebellar cortex, moderate astrogliosis was present in the deep cerebellar nuclei (B), and pronounced astrogliosis was present in the cerebral cortex (C). Purkinje cells were sparse in the cerebellum of dog B, but structures resembling the clusters of autofluorescent cells were present in the Purkinje layer (arrow in A). Purkinje cell densities were greater in Dog C. Aggregates of hematoxylin-stained material were present in the cell bodies on large neurons in the deep nuclei of the cerebellum (arrowheads in B). Bar in (C) indicates the magnification of all 3 micrographs.

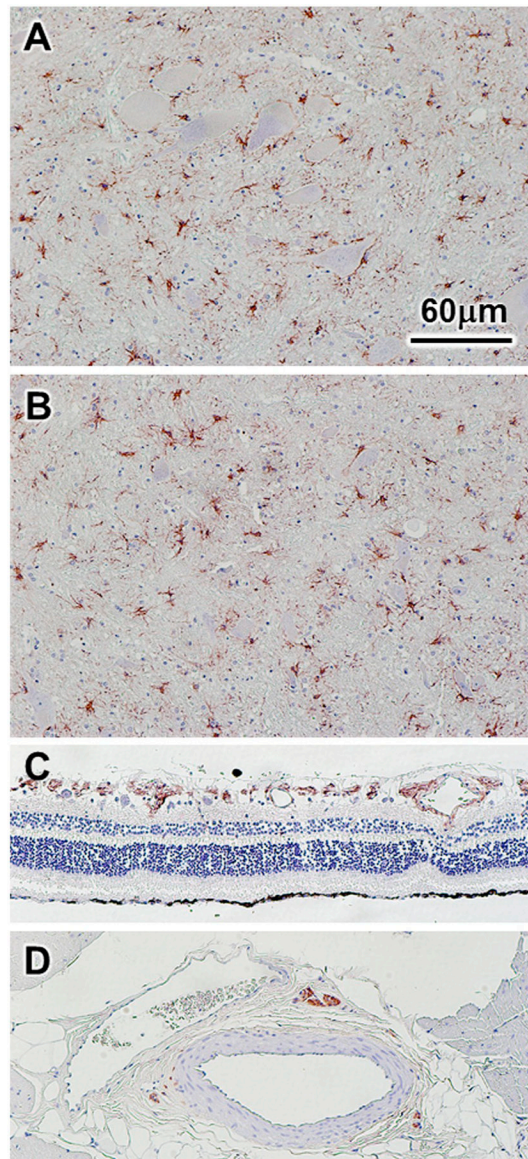
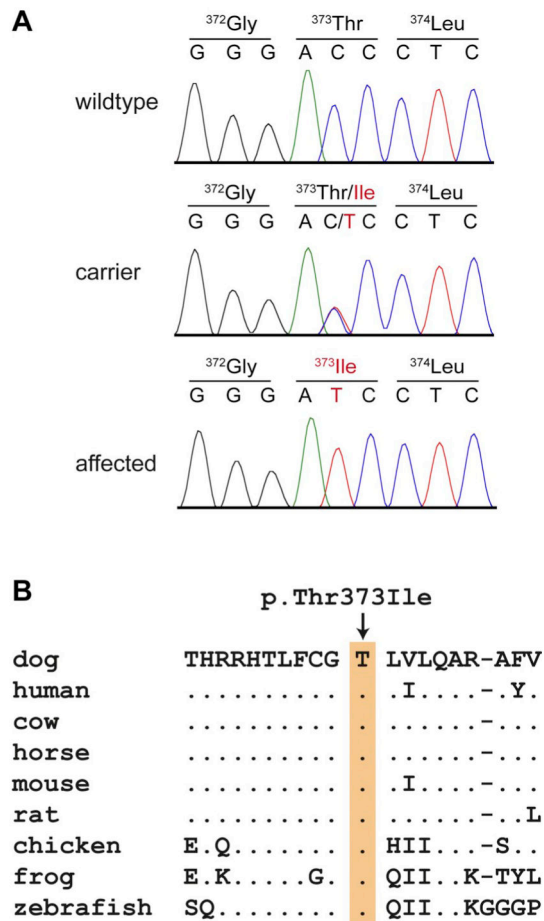


Fig. 13. GFAP IHC stained sections of cervical spinal cord ventral horn (A), cervical spinal cord dorsal horn (B), retina (C), and large cardiac ventricular muscle blood vessel from affected dog C. Significant astrogliosis was observed throughout the spinal cord gray matter (A and B) and in the retinal ganglion cell layer (C). GFAP-stained cells were also observed adjacent to blood vessels in the cardiac ventricular wall muscle (D). Bar in (A) indicates the magnification of all 4 micrographs.

**Fig. 14.**

Details of the *ATP13A2*:c.1118C > T variant. (A) Sanger electro-pherograms from dogs with the three different genotypes confirm the presence of the variant. (B) A multiple species alignment of the *ATP13A2* amino acid sequence illustrates that the variant affects a highly conserved region of the protein. The wildtype threonine is perfectly conserved across diverse vertebrates.

Table 1

Variants detected by whole genome resequencing of an affected Australian Cattle Dog.

Filtering step	Variants ^a
Variants in whole genome	4,028,278
Private variants in the whole genome ^b	20,975
Private protein changing variants in the whole genome	151
Private protein changing variants in 12 candidate genes ^c	1

^aOnly variants which passed the GATK quality filter were counted.

^bPrivate variants were exclusively present in the affected dog and had homozygous reference or missing genotype calls in 217 control genomes.

^c*ATP13A2, CLN3, CLN5, CLN6, CLN8, CTSD, CTSF, DNAJC5, GRN, MFSD8, PPT1, TPP1* (Table S1).

Table 2Association of the *ATP13A2:c.1118C > T* genotypes with neuronal ceroid lipofuscinosis.

Genotype	C/C	C/T	T/T
Affected Australian Cattle Dogs (<i>n</i> = 3)	-	-	3
Australian Cattle Dogs, unaffected or population controls (<i>n</i> = 394)	352	42	-
Dogs from other breeds	555	-	-

Author Manuscript

Author Manuscript

Author Manuscript

Author Manuscript